Tetrahedron 65 (2009) 4332–4339

Contents lists available at ScienceDirect

Tetrahedron

journal homepage: www.elsevier.com/locate/tet

Fine tuning of molecular rotor function in photochemical molecular switches

Matthijs K.J. ter Wiel, Ben L. Feringa *

Department of Organic Chemistry, Stratingh Institute for Chemistry, University of Groningen, Nijenborgh 4, 9747 AG Groningen, The Netherlands

ARTICLE INFO

Article history:
Received 30 July 2008
Received in revised form 8 March 2009
Accepted 26 March 2009
Available online 1 April 2009

ABSTRACT

Molecular switches are used as scaffolds for the construction of controlled molecular rotors. The internal position of the switching entity in the molecule controls the dynamic behaviour of the rotor moiety in the molecule. Six new molecular motors with *o*-xylyl rotor moieties were prepared on the basis of an overcrowded alkene, and their dynamics were systematically studied by 2D EXSY NMR. Variation of the (hetero-)atoms in the upper and lower halves of the overcrowded alkene allows fine tuning of the rate of rotation of the *o*-xylyl rotor in the lower half of the molecule. For all rotors it was observed that the rotation barrier for the trans-isomer was higher than that of the corresponding cis-isomer. The results are analyzed and discussed in terms of differences in steric interactions in the presented system.

1. Introduction

The design of an artificial molecular system that functions as a tiny machine requires precise control over the mechanical movements of its components.[1] The fascinating biological linear and rotary motors found in natural systems offer a major source of inspiration, and the complexity of their structures encourages us to conceptualize the principles and build entirely synthetic molecular machines.[2] The control over the dynamics and motions in molecular and supramolecular systems is one of the great contemporary challenges, which might lead to considerable advances in the field of molecular nanotechnology.[3–5] Remarkable progress has been made in the control of rotary motion in molecular rotors[6] and in the design of a variety of more elaborate, but still rather primitive mimics of common machinery such as molecular motors,[7] elevators,[8] muscles,[9] scissors[10] and gyroscopes.[11]

An important starting point for the construction of most of these devices is to restrict the internal rotational degrees of freedom within the molecule. This is especially true in the case of a molecular rotor, which is according to the definition of Michl et al. "a molecular system in which a molecule or a part of a molecule rotates against another part of the molecule or against a macroscopic entity such as a surface or a solid".[6]

Our efforts to construct molecular machinery have focused on the application of the unique properties of overcrowded alkenes. We have shown that in molecular motors derived from these molecules a repetitive, 360°, unidirectional rotary motion can occur by selective movement of the upper part relative to the lower part of the molecule by irradiation and heating.[7a,12] In molecular switches based on overcrowded alkenes, control over the position and movement over 180° of the upper part relative to the lower part are exerted by irradiation with light of different wavelengths.[13] Using the concepts of molecular motors[14] and switches,[15] we designed a system in which two distinct rotating units are coupled in their movement. We envisioned that the stereochemical restrictions of the movement of a molecular motor or molecular switch can be used to exert control over the dynamics of a rotor entity in such a molecular system. In molecular rotor **1**, the speed of rotation around the aryl–aryl single bond is varied by changing the configuration of the central alkene and simultaneously the position of its naphthalene upper part (Fig. 1).

In the overcrowded alkene **1**, the lower part of the molecule has been used as a scaffold to attach a rotating *o*-xylyl unit.[15] Due to the proximity of the upper half of the molecule, this *o*-xylyl moiety is not rotating freely, but is restricted in its movement. On the NMR time scale well resolved signals are observed for the methyl groups of both *cis*-**1** and *trans*-**1** isomers of the *o*-xylyl rotor. The rotation of

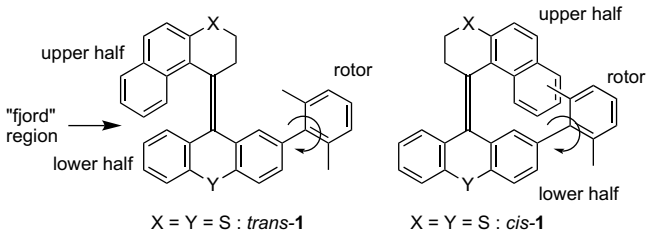

Figure 1. Trans- and cis-isomers of molecular rotor **1**.

* Corresponding author. Tel.: +31 50 363 4278; fax: +31 50 363 4296.
E-mail address: b.l.feringa@rug.nl (B.L. Feringa).

0040-4020/$ – see front matter © 2009 Elsevier Ltd. All rights reserved.
doi:10.1016/j.tet.2009.03.081

biaryl units is slow at ambient temperatures, and no coalescence temperature could be attained for either isomer of **1**. However, EXSY spectroscopy allowed an accurate determination of the rotation barriers. Although it was anticipated that due to the spatial orientation of the naphthalene moiety the rate of rotation for *trans*-**1** would be faster than *cis*-**1**, it was surprisingly found that the speed of rotation in *cis*-**1** was significantly higher. It therefore appeared that as if a single methylene group was more sterically demanding than a naphthalene group. These unexpected findings were confirmed by AM1 calculations performed for this molecule.

To further address this remarkable, and counterintuitive phenomenon, we present here a systematic investigation of structural parameters, and in particular address the influence of the (hetero-) atoms X and Y in the crucial bridging positions in upper and lower halves on the rate of rotation of the *o*-xylyl rotor. In total, six molecular rotors were prepared by combining three upper halves (X=S, O and CH_2) with two lower halves (Y=S and O). Their thermodynamic data were obtained by measuring the kinetics of the biaryl rotation by EXSY spectroscopy.

2. Results

The molecular rotors **1**–**6** were synthesized according to previously described methodology for the construction of these overcrowded alkenes.[16] The key step in the synthesis of these molecules, depicted in Scheme 1, is the formation of the central double bond via a two-fold extrusion process. In this diazo-thioketone coupling of upper and lower halves, an in situ generated diazo compound is reacted with a thioketone in a 1,3-dipolar cycloaddition to yield a thiadiazoline. These intermediates are not stable, and rapidly eliminate nitrogen to give the corresponding episulfides. In the final step of the synthesis, the sulfur atom is extruded by heating the episulfides at reflux in toluene or *p*-xylene in the presence of copper powder or triphenylphosphine.

Molecular rotor **1** was prepared according to the published procedure.[15] This procedure was similarly employed for the synthesis of molecular rotors **2**–**6**. The required hydrazones for the upper half, **7** (X=S), **8** (X=CH_2) and **9** (X=O), were synthesized according to literature procedures.[17] Similarly, the thioxanthone lower half **10**, containing a sulfur atom in the Y position, was prepared according to the literature procedure.[15] For the xanthone lower half **11** (Y=O), no literature precedent existed, and a synthetic route was devised starting from 2-bromoxanthone **12**.[18] Attachment of the *o*-xylyl moiety was accomplished by employing a Suzuki coupling with 2,6-dimethylphenylboronic acid **13** and $Pd(PPh_3)_4$, using $Ba(OH)_2$ as base in a solvent mixture of DME and water. Conversion to the thioketone **11** was readily performed by treating ketone **14** with P_4S_{10} in toluene at reflux.

Oxidation of the hydrazones **7**, **8** and **9** to the corresponding diazo compounds was accomplished using Ag_2O as oxidant and KOH as base in the presence of $MgSO_4$ in CH_2Cl_2. These in situ generated diazo compounds were reacted in a 1,3-dipolar cycloaddition with the two thioketones **10** and **11** to yield episulfides **15**–**19** in low to excellent yields (17–97%). The varying yields are mainly due to the unpredictable nature of the oxidation reaction of the hydrazones using Ag_2O, the outcome being strongly substrate dependant. Meanwhile, a more convenient procedure has been developed in our laboratory using [bis(trifluoroacetoxy)iodo]benzene.[19] Sulfur extrusion could be cleanly effected by heating the episulfides **15**–**19** in boiling *p*-xylene in the presence of copper powder to provide the rotor molecules **2**–**6** in high yields (80–98%). In all cases, a small preference for the formation of the cis-isomer over the trans-isomer was found.

The naphthalene upper part of the alkenes **1**–**6** adopts either a cis- or a trans-geometry with respect to the rotor in the lower half of the molecule. The rotor part therefore experiences a different environment for each isomer. Both geometrical isomers of **1**–**6** were readily distinguished by the difference in absorptions in the ^{1}H NMR spectra of the methyl groups of rotor part. For the cis-isomers, the difference in the ^{1}H NMR absorptions is relatively large, as can be seen, for example, for *cis*-**1**: δ 0.71 and δ 1.72 ppm. One methyl substituent experiences a large influence of the ring current anisotropy of the upper half naphthalene moiety, whereas this influence is much smaller for the other methyl substituent (Fig. 1). For the *trans*-**1** isomer, the difference in chemical shift for the two methyl substituents is much smaller (δ 1.98 and δ 2.23 ppm), as the deshielding naphthalene moiety is farther away. As stated above, previous NMR experiments performed with rotor **1** showed that the energy barriers for the rotation of the *o*-xylyl moiety were too high to be accurately determined by coalescence of the ^{1}H NMR signals. Since 2D EXSY experiments were successfully performed with rotor **1** and the activation energies for the newly synthesized rotors **2**–**6** were expected to be in the same range, we decided to perform EXSY measurements on these new rotors to quantify the thermodynamic parameters for the dynamics of the rotor function.[20]

The *o*-xylyl moiety of the rotor part is well suited for EXSY experiments, since it behaves as a two-site exchange system. The advantages of this two-state system are that the populations are equal and that the spin–lattice relaxation time is, within error margins, the same for both methyl substituents. It is important to record at each temperature, spectra with different mixing times

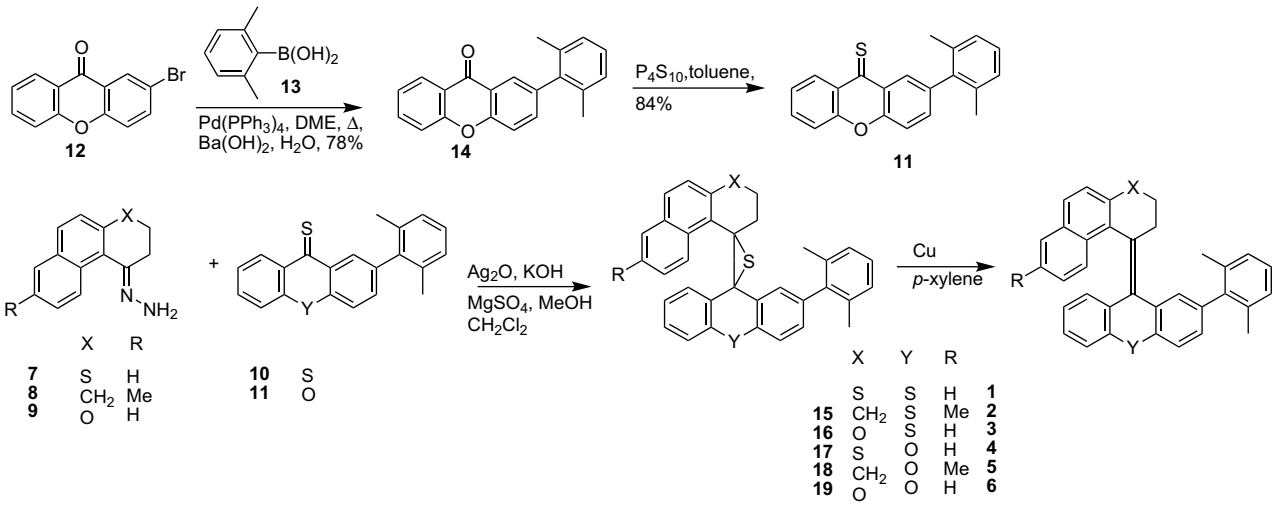

Scheme 1. Synthesis of molecular rotors **1**–**6** featuring a two-fold extrusion process for the formation of the central double bond.

(t_m) in order to measure the exchange process in the initial rate regime (the NOE signal build-up and decay have ideally a bell shape).[21] Recording NOESY spectra is time consuming and in order to save time the measurements were performed on a mixture of *cis*-**1**–**6** and *trans*-**1**–**6**. Moreover, this also ensured identical measuring conditions for the cis- and trans-isomers allowing direct comparison. The EXSY spectra were recorded at 25, 35, 45 and 55 °C.[22] At each temperature different mixing times (typical values of t_m were 0.05, 0.1, 0.2, 0.3, 0.5, 0.7, 1.0 and 1.5 s)[23] were used, and care was taken to use only data obtained in the initial rate regime. Where possible, the average value of the two cross-peaks a_{AB} and a_{BA} was used in order to minimize the error margin. However, for the trans-isomers of rotors **4** and **5**, both with an oxygen atom in the lower half, no accurate data could be obtained due to overlap with the proton absorptions of protons of the six-membered ring in the upper half of the molecule. From the slope of the plot of t_m versus $(a_{AB}/(a_{AA}+a_{AB}))$, the rate constant k for the rotation at each temperature was determined for all cis-isomers and all but the previously mentioned two trans-isomers. These rates are depicted for various temperatures in Figures 2 and 3.[24]

In Figures 2 and 3, the rates of rotation for all cis- and nearly all trans-rotors **1**–**6** are depicted. At lower temperatures (25 and 35 °C), the rates of rotation were all within a close range, but at higher temperatures (45 and 55 °C) the differences became more pronounced. At 55 °C the order of the rate of rotation was going from a slow to a fast rate of rotation: *trans*-**1** (S,S)<*trans*-**2** (C,S)<*trans*-**3** (O,S)<*trans*-**1** (O,O)<*cis*-**3** (O,S)<*cis*-**2** (C,S)<*cis*-**5** (C,O)<*cis*-**1** (S,S)<*cis*-**6** (O,O)<*cis*-**4** (S,O). From the rate constants determined by EXSY spectroscopy, the thermodynamic parameters associated with the activation barrier could be determined using an Eyring plot. The values of these thermodynamic data are summarized in Table 1 and more data are provided in Supplementary data.

In order to visualize the differences in the thermodynamic parameters, the Eyring plots of both cis- and trans-isomers of the rotors **1**, **2** and **3** are depicted in Figure 4.

3. Discussion

The most apparent feature of this system is that in all cases the trans-isomers rotate slower than the respective cis-isomers (Figs. 2 and 3). This remarkable behaviour was also observed and investigated in detail for rotor **1**.[15] It was found that in the transition state of the rotation of the *o*-xylyl moiety for the cis-isomer of **1**, the naphthalene moiety bends away and hence facilitates the rotation in the lower half of the molecule. For the *trans*-**1** isomer, it is proposed that in the transition state, the methyl protons of the rotor become entangled in the ring protons of the upper half of the molecule, leading to a lower rate of rotation in comparison to the *cis*-**1** isomer.

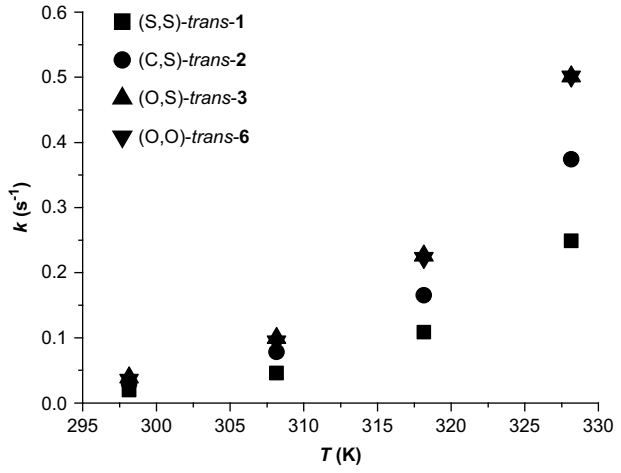

Figure 2. Rates of rotation for all measured trans-isomers of the rotors. In brackets (X,Y) are indicated the (hetero-)atoms in the upper (X) and lower halves (Y).

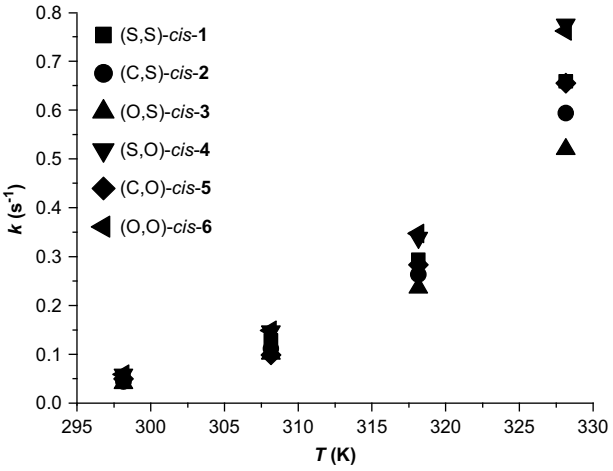

Figure 3. Rates of rotation for all measured cis-isomers. In brackets (X,Y) are indicated the (hetero-)atoms in the upper (X) and lower halves (Y).

By introduction of various hetero-atoms in the upper and lower half, the steric crowding in the molecule can be directly influenced, which has a direct impact on the speed of the rotation of the *o*-xylyl moiety. The hetero-atoms on the bridging positions are important for the shape of the molecule. Large atoms like sulfur will push the aromatic moieties more towards each other than the smaller oxygen atoms, leading to an increase in steric crowding in the so-called '*fjord-region*' of the molecule.

This can be seen by comparison of the bond lengths in the molecule; bond lengths of an aromatic ether (C–O) and aromatic thioether (C–S), as are present in the lower half, were found to be 1.39 Å and 1.77 Å (based on X-ray data) for similar molecules.[25] In the upper half, these bond lengths are for $C_{3'}$–$O_{4'}$–$C_{4'a}$ (1.45 and 1.36 Å), for $C_{1'}$–$C_{2'}$–$C_{10'}$ (1.55 and 1.52 Å) and finally for $C_{3'}$–$S_{4'}$–$C_{4'a}$ (1.82 and 1.77 Å). The behaviour of the rotors **1**–**6** is readily explained on the basis of steric hindrance and the bond lengths of the different atoms (O, C, S). Since the length of the carbon–carbon bonds is approximately in-between the length of carbon–oxygen and carbon–sulfur bonds, the effect on the rate of rotation is expected to result in values in between those of sulfur and oxygen containing rotors.

All cis- and trans-isomers of rotors **1**–**3** that contain a sulfur atom in the lower half could be measured by 2D EXSY experiments. It was expected that the *cis*-**1** (S,S) rotor would rotate slower than *cis*-**2** (C,S) and *cis*-**3** (O,S), since the larger sulfur atom would push

Table 1
Thermodynamical data for rotors **1**–**6**

	$\Delta^{\ddagger}G^{\theta}$ (kJ mol^{-1})[a]	$\Delta^{\ddagger}H^{\theta}$ (kJ mol^{-1})	$\Delta^{\ddagger}S^{\theta}$ (J K^{-1} mol^{-1})
cis-**1** (S,S)	80±1	67.4±0.8	−43±3
trans-**1** (S,S)	82±2	66±1	−57±4
cis-**2** (C,S)	80.5±0.2	67.8±0.1	−43.2±0.3
trans-**2** (C,S)	81±2	65±2	−54±6
cis-**3** (O,S)	80.7±0.2	66.3±0.2	−49.0±0.5
trans-**3** (O,S)	81±1	66.3±0.7	−49±2
cis-**4** (S,O)	79.8±0.7	67.1±0.5	−43±2
trans-**4** (S,O)	[b]	[b]	[b]
cis-**5** (C,O)	80±1	67±1	−44±3
trans-**5** (C,O)	[b]	[b]	[b]
cis-**6** (O,O)	79.8±0.6	66.8±0.5	−44±1
trans-**6** (O,O)	81±1	68.8±0.7	−41±2

In brackets (X,Y) are indicated the (hetero-)atoms in the upper (X) and lower halves (Y).
[a] T=293.15 K.
[b] No data could be obtained due to overlap in the ^{1}H NMR spectrum.

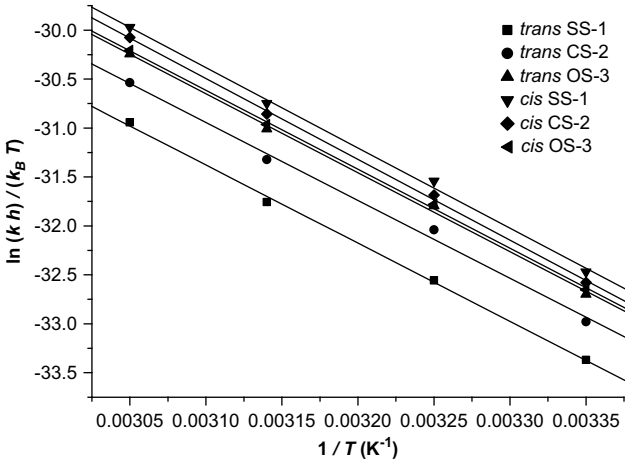

Figure 4. Eyring plots for the rotors **1**, **2**, and **3** containing a sulfur atom in the lower half of the molecule.

the upper half naphthalene more towards the rotor than the smaller carbon and oxygen atoms. However, it was found that *cis*-**1** (S,S) rotated faster than *cis*-**2** (C,S) and *cis*-**3** (O,S), which had the slowest rate of rotation. Apparently, the large sulfur atom in the upper half of *cis*-**1** (S,S) bends the naphthalene moiety farther away from the rotor part, and hence an increased rate of rotation is observed compared to *cis*-**2** and *cis*-**3** with carbon and oxygen atoms in the upper half. For the rate of rotation of the trans-isomers, this sequence is reversed and the rate decreases from *trans*-**3** (O,S) to *trans*-**2** (C,S) and *trans*-**1** (S,S). It appears as if the large sulfur atom in the upper half of *trans*-**1** (S,S) pushes the two protons at $C_{2'}$, hence in the α position with respect to the double bond, towards the rotor part in the lower half. A more dramatic result is to be expected when the sulfur atoms are replaced by coordinated metal ions like zinc or palladium, as we have demonstrated for similar systems.[26] In the case of *trans*-**2** (C,S) and *trans*-**3** (O,S) the steric hindrance is partly relieved and this results in an increased rate of rotation of the rotor. On the basis of steric hindrance, the expected order in the rate of rotation is therefore observed: *trans*-**3** (O,S)>*trans*-**2** (C,S)>*trans*-**1** (S,S). Notable is the small difference in the rate of rotation found between the *cis*-**3** (O,S) and *trans*-**3** (O,S).

Results obtained for the system with a lower half containing an oxygen atom were less consistent and more difficult to interpret, since no EXSY data could be obtained for *trans*-**4** (S,O) and *trans*-**5** (C,O) due to the overlap of NMR absorptions of the rotor methyl groups with the protons of the upper ring of the molecule. When the argumentation used to explain the different rates of rotation of the cis-isomers with sulfur atoms in the lower half is applied to the cis-isomers with an oxygen atom in the lower half, the *cis*-**4** (S,O) and *cis*-**5** (C,O) isomer being substituted with an oxygen atom display similar behaviour. *cis*-**4** (S,O) rotates faster than *cis*-**5** (C,O), as the upper half of *cis*-**4** (S,O) is pushed away further, allowing a higher speed compared to *cis*-**5** (C,O). *cis*-**4** (S,O) and *cis*-**5** (C,O) have a slightly increased rate of rotation relative to their sulfur analogues *cis*-**1** (S,S) and *cis*-**2** (C,S). The oxygen atoms in the lower half pull the lower part with the rotor better away from the sterically demanding region and therefore a higher rate of rotation is observed for all oxygen-substituted compounds compared to their sulfur substituted counterparts.

Not in line with the results for all other rotor molecules is the behaviour of *cis*-**6** (O,O), containing an oxygen in both upper and lower halves. This *cis*-**6** (O,O) rotor shows faster rotation than *cis*-**5** (C,O) and is only marginally slower in its rotation than *cis*-**4** (S,O). On the basis of results shown above, it would have been expected that a sulfur or carbon atom would have pushed the lower half farther away than an oxygen atom and allow much faster rotation for *cis*-**4** (S,O) and *cis*-**5** (C,O) compared to *cis*-**6** (O,O). The only viable explanation is that the steric hindrance in *cis*-**6** (O,O) is lowered to such an extent by contraction of the upper and lower halves that the naphthalene moiety is bent much farther away from the rotor part allowing a higher rate of rotation. For the trans-isomers substituted in the lower half with oxygen, only *trans*-**6** (O,O) could be studied. Compared to *trans*-**3** (O,S), only a small rate enhancement for *trans*-**6** (O,O) was observed, which is in agreement with the explanation given above for molecular rotors with a sulfur atom in their lower halves.

Although in general a clear difference in rate of rotation is observed for the different isomers of the molecular rotors **1**–**6**, the observed activation barriers are comparable. This makes a discussion difficult using the data that have been obtained from the Eyring plots, especially since not for all rotors data became available (two trans-rotors could not be measured). At room temperature the Gibbs energy of activation for the rotation process is similar for all molecules, which is obvious taking into account the slow rate of rotation of all rotor systems at lower temperatures. However, as can be seen more clearly from Table 1 and Figure 4, the differences in rate of rotation can be accounted for in terms of enthalpic and entropic effects. The enthalpy of rotation is in the range of 65±2 to 68.8±0.7 kJ mol^{-1} and is for all rotors more or less the same. However, considering only the more complete dataset of rotors containing a sulfur atom in the lower half, one can see clearly that the enthalpy of rotation stays largely the same, while the entropy of rotation causes the differences in the rate of rotation. This effect is most pronounced for rotors *cis*-**1** ($\Delta^{\ddagger}S^{\theta}=-43\pm3$ J K^{-1} mol^{-1}) and *trans*-**1** ($\Delta^{\ddagger}S^{\theta}=-57\pm4$ J K^{-1} mol^{-1}), gets lesser in the *cis*-**2** ($\Delta^{\ddagger}S^{\theta}=-43.2\pm0.3$ J K^{-1} mol^{-1}) and *trans*-**2** ($\Delta^{\ddagger}S^{\theta}=-54\pm6$ J K^{-1} mol^{-1}), and as the entropy is nearly the same for the rotors *cis*-**3** ($\Delta^{\ddagger}S^{\theta}=-49.0\pm0.5$ J K^{-1} mol^{-1}) and *trans*-**3** ($\Delta^{\ddagger}S^{\theta}=-49\pm2$ J K^{-1} mol^{-1}): they nearly rotate at the same rate. Visually this is depicted in Figure 4, in which for all six rotors the same slope was obtained in the respective Eyring plots, but a difference intercept was obtained.

4. Conclusions

We have effectively demonstrated that the rate of rotation of an *o*-xylyl rotor moiety attached to the lower half of the molecule can be manipulated effectively by variation of the (hetero-)atoms X and Y in the upper and lower halves of the rotor molecules **1**–**6**. In all cases, the rates of rotation of the cis-isomers **1**–**6** were higher than the (corresponding) trans-isomers **1**–**6**. This in agreement with previous findings and can be accounted for by the difference in steric hindrance. For the trans-isomers, the methyl protons of the *o*-xylyl rotor become entangled with the methylene protons of the upper half, leading to a high energetic barrier in the transition state. For the cis-isomers, this energetic barrier is lower, since during the *o*-xylyl rotation the naphthalene upper part can bend away effectively.

The rotors **1**–**3** with a sulfur atom in the lower half are most easily compared. All cis- and trans-isomers of **1**, **2** and **3** could be measured by EXSY NMR. For two trans-isomers (*trans*-**4** and *trans*-**5**) of the oxygen-substituted rotors (Y=O) no data could be gathered, as the methyl absorptions of the rotor overlapped with those of protons in the upper part of the molecule. The rate of rotation observed was for all rotors: *trans*-**1** (S,S)<*trans*-**2** (C,S)<*trans*-**3** (O,S)<*trans*-**1** (O,O)<*cis*-**3** (O,S)<*cis*-**2** (C,S)<*cis*-**5** (C,O)<*cis*-**1** (S,S)<*cis*-**6** (O,O)<*cis*-**4** (S,O). For the trans-isomer **1**–**3** the expected rate differences are readily accounted for on the basis of steric hindrance. The larger sulfur atoms bend the rotor more towards the upper part, and the methyl substituents of the rotor become entangled with the protons of the upper ring. The observed increase in the rate of rotation is therefore logically determined by

the size of the bridging atoms: *trans*-**1** (S,S), *trans*-**2** (C,S) and trans-**3** (O,S). It was remarkable to see that the *cis*-**1** (S,S) rotated faster than *cis*-**3** (O,S) and *cis*-**2** (C,S). This, however, can be explained by noting that the 'bigger' sulfur atom bends the naphthalene moiety away more effectively in the transition state, leading to a higher rate of rotation. For the rotors containing a sulfur atom in the lower half, it could be shown that the differences in speed are caused by the differences in the entropy of activation for the rotation process. These entropic effects follow the reasoning that was given on the basis of steric effects, the trans-isomers being more hindered than the cis-isomers, as well as the decrease in atom size going from sulfur to carbon, and finally oxygen.

Comparison of the rotors containing oxygen in the lower half was more difficult since not all data could be obtained. All oxygen-substituted *cis*-isomers **4**–**6** rotated faster than the respective sulfur substituted rotors **1**–**3**. However, the behaviour of the *cis*-**6** (O,O) was unexpected since its rotation should have been much slower than that of *cis*-**5** (C,O) and *cis*-**4** (S,O).

Currently, investigations are underway to control the movement of the upper part relative to the rotor by introducing a different substitution patterns on the lower half of the molecule. This might allow manipulation of the rate of movement at the molecular level by irradiation with light.

5. Experimental section

5.1. General

The high-resolution one- and two-dimensional ^{1}H NMR spectra were obtained using a Varian VXR-300, and a Varian Unity Plus Varian-500 operating at 299.97 and 499.86 MHz, respectively, for the ^{1}H nucleus. ^{13}C NMR spectra were recorded on a Varian VXR-300 operating at 75.43 MHz. Chemical shifts are reported in δ units (ppm) relative to the solvent signals of $CHCl_3$ (^{1}H NMR: δ 7.26 ppm) and $CDCl_3$ (^{13}C NMR: δ 77.0 ppm). The splitting patterns are designated as follows: s (singlet), d (doublet), t (triplet), q (quartet), and m (multiplet). One-dimensional ^{1}H NMR spectra were recorded using the acquisition parameters: $\pi/2$ pulse width, 6.5 μs; spectral width, 6.000 Hz; data size, 16 K; recycling delay, 1 s; number of transients, 32; temperature 298 K. COSY,[27] clean-TOCSY (MLEV-17),[28] NOESY[21a] and HMQC[29] experiments were used for the assignment of the ^{1}H and ^{13}C NMR resonances when required.[30] All 2D spectra were collected as 2D hyper-complex data. After weighting with shifted sine-bell functions, the COSY data were Fourier transformed in the absolute value mode using standard Varian VnmrS/VnmrX software packages. COSY and TOCSY spectra were accumulated typically with 256 increments and 32 scans per increment. Two-dimensional phase-sensitive ^{1}H–^{1}H chemical shift correlation spectra with double quantum filter (DQF-COSY)[31] were obtained with the acquisition parameters: $\pi/2$ pulse width, 6.5 μs; spectral width, 6.000 Hz; recycling delay, 1.0 s. The data were 512 W in the F1 dimension and 1 K in the F2 dimension and were zero-filled in F1 prior to two-dimensional Fourier transformation to yield a 1 K×1 K data matrix. The spectra were processed using shifted sine-bell window functions in both dimensions.

Two-dimensional phase-sensitive ^{1}H–^{1}H nuclear Overhauser enhancement spectra (NOESYPH)[20] for NMR exchange experiments were collected at 500 MHz using the acquisition parameters similar to the DQF-COSY. Typically, 1024 increments and 4 scans per increment were accumulated applying a relaxation delay of 1.0 s. The measurements were conducted at 25, 35, 45 and 55 °C consisting of an arrayed cluster of mixing times (t_m=0.05, 0.1, 0.2, 0.3, 0.5, 0.7, 1.0 and 1.5 s) per temperature.[23,32,33] The initial rate approximation was used for calculation of rate constants[30] for the case of slow exchange between two equally populated sites and in the absence of scalar (*J*-modulated) spin–spin coupling. Peak integrals were determined by means of integration of the cross- (a_{AB} and a_{BA}) and auto-signals (a_{AA} and a_{BB}).

Melting points were taken on a Mettler FP-2 melting point apparatus, equipped with a Mettler FP-21 microscope. Optical rotations were measured with a Perkin Elmer 241 Polarimeter. UV–vis measurements were performed on a Hewlett–Packard HP 8453 FT spectrophotometer and CD spectra were recorded on a JASCO J-715 spectropolarimeter using Uvasol grade solvents (Merck). MS (EI) and HRMS (EI) spectra were obtained with a Jeol JMS-600 spectrometer. Elemental analyses were performed in the microanalytical department with a Foss-Heraeus CHN-O-Rapid or a EuroVector Euro EA Elemental Analyzer. The average value of duplo measurements is reported. Column chromatography was performed on silica gel (Aldrich 60, 230–400 mesh). Solvents were distilled and dried before use by standard methodology. Chemicals were used as-received from Acros, Aldrich, Fluka or Merck.

5.2. General procedure for the synthesis of alkenes 2–6

A solution of the cis–trans mixture of episulfides **15**–**19** in *p*-xylene (10 ml) was heated at reflux overnight in the presence of copper powder (2 or 3 molar equiv relative to the episulfide). After cooling, the reaction mixture was filtered and the residue washed with CH_2Cl_2. All volatiles were removed under reduced pressure providing the crude alkenes **2**–**6** ready for further purification by column chromatography.

*5.2.1. 2-(2,6-Dimethylphenyl)-9-(7′-methyl-2′,3′-dihydro-4′(1′H)-phenanthren-4′-ylidene)-9H-thioxanthene (**2**)*

The episulfide **15** (80 mg, 0.15 mmol) was treated with copper powder (200 mg) in *p*-xylene using the standard procedure giving alkene **2** as a colourless oil (60 mg, 0.12 mmol, 80%). Purification was performed by column chromatography (SiO_2, heptane/ethyl acetate=50:1); ^{1}H (500 MHz, $CDCl_3$) δ 0.74 (s, 3H, cis), 1.78 (s, 3H, cis), 1.93–2.42 (m, 3H, cis; 3H, trans), 2.05 (s, 3H, trans), 2.31 (s, 3H, trans), 2.39 (s, 3H, trans), 2.42 (s, 3H, cis), 3.00–3.16 (m, 2H, cis; 2H, trans), 3.38–3.48 (m, 1H, cis; 1H, trans), 6.36–6.37 (d, *J*=1.5 Hz, 1H), 6.42–6.50 (m, 2H), 6.60–6.63 (dd, *J*=8.1, 1.8 Hz, 1H), 6.83–7.72 (m, 26H); ^{13}C (75 MHz, $CDCl_3$) δ 19.3 (q), 20.7 (q), 21.0 (q), 21.1 (q), 21.2 (q), 21.3 (q), 22.1 (t), 22.2 (t), 28.2 (t), 28.6 (t), 124.8 (d), 125.0 (d), 125.4 (d), 125.7 (s), 125.9 (d), 126.1 (d), 126.4 (d), 126.6 (d), 126.65 (d), 126.68 (d), 126.73 (d), 126.80 (d), 126.83 (d), 127.0 (d), 127.2 (d), 127.37 (d), 127.44 (d), 127.52 (d), 127.56 (d), 128.2 (d), 128.5 (d), 128.6 (d), 128.7 (d), 132.0 (s), 132.2 (s), 132.3 (s), 132.7 (s), 132.8 (s), 133.7 (s), 133.8 (s), 133.9 (s), 134.2 (s), 135.1 (s), 135.8 (s), 135.9 (s), 136.1 (s), 136.3 (s), 136.4 (s), 136.47 (s), 136.50 (s), 136.7 (s), 136.8 (s), 137.02 (s), 137.07 (s), 137.12 (s), 138.6 (s), 138.8 (s), 139.0 (s), 139.2 (s), 140.8 (s), 141.2 (s), due to overlap in the aromatic region of the spectrum eight (d) and two (s) signals were not observed; *m*/*z* (EI, %)=494 (M^+, 100); HRMS (EI) calcd for $C_{36}H_{30}S$: 494.2068, found: 494.2078.

*5.2.2. 2-(2,6-Dimethylphenyl)-9-(2′,3′-dihydro-1′H-naphtho-[2,1-b]pyran-1′-ylidene)-9H-thioxanthene (**3**)*

Heating at reflux of the episulfide **16** (60 mg, 0.11 mmol) in *p*-xylene in the presence of copper powder (200 mg) gave the alkene **3** as a colourless oil. After purification by column chromatography (SiO_2, heptane/ethyl acetate=50:1) the oil solidified upon standing and after washing with ether alkene **3** was obtained as a white solid (54 mg, 0.11 mmol, 96%); ^{1}H (500 MHz, $CDCl_3$) δ 0.70 (s, 3H, cis), 1.72 (s, 3H, cis), 1.95 (s, 3H, trans), 2.21 (s, 3H, trans), 2.47–2.53 (m, 1H, cis), 2.60–2.67 (m, 1H, trans), 3.56–3.61 (m, 1H, cis; 1H, trans), 4.60–4.66 (m, 1H, trans), 4.67–4.72 (m, 1H, cis), 4.84–4.87 (m, 1H, trans), 4.90–4.93 (m, 1H, cis), 6.49–6.52 (t, *J*=7.2 Hz, 1H, trans), 6.64–7.69 (m, 16H, cis; 15H, trans); ^{13}C (75 MHz, $CDCl_3$) δ 19.6 (q), 20.7 (q), 20.9 (q), 21.1 (q), 29.0 (t), 29.3 (t), 69.6 (t), 69.7 (t), 117.8 (s),

118.0 (s), 118.1 (d), 118.5 (d), 122.6 (d), 122.9 (d), 124.4 (d), 124.5 (d), 125.3 (d), 125.5 (d), 126.0 (d), 126.3 (d), 126.6 (d), 126.7 (d), 126.8 (d), 126.9 (d), 127.3 (d), 127.4 (d), 127.5 (d), 127.6 (d), 127.67 (d), 127.71 (d), 127.8 (d), 128.46 (s), 128.54 (s), 129.06 (d), 129.3 (d), 129.92 (s), 130.9 (s), 131.4 (s), 133.1 (s), 134.2 (s), 134.6 (s), 135.9 (s), 136.0 (s), 136.3 (s), 136.36 (s), 136.44 (s), 136.7 (s), 138.6 (s), 139.1 (s), 139.2 (s), 139.4 (s), 140.6 (s), 154.09 (s), 154.14 (s). Due to overlap in the aromatic region of the spectrum only 24 out of 32 signals for doublets and 22 out of 28 signals for singlets were observed; *m*/*z* (EI, %)=482 (M^+, 100); HRMS (EI): calcd for $C_{34}H_{26}OS$: 482.1704, found: 482.1697.

5.2.3. 2-(2,6-Dimethylphenyl)-9-(2′,3′-dihydro-1′H-naphtho-[2,1-b]thiopyran-1′-ylidene)-9H-xanthene (**4**)

Starting from episulfide **17** (120 mg, 0.23 mmol) using the standard procedure with *p*-xylene and copper powder, the alkene **4** (110 mg, 0.23 mmol, 98%) was obtained as a white solid after column chromatography (SiO_2, heptane/ethyl acetate=50:1); ^1H (300 MHz, $CDCl_3$) δ 0.77 (s, 3H, cis), 1.71 (s, 3H, cis), 2.02 (s, 3H, trans), 2.00–2.28 (m, 1H, cis; 1H, trans), 2.26 (s, 3H, trans), 3.40–3.58 (m, 2H, cis; 2H, trans), 3.77–3.87 (m, 1H; cis, 1H, trans), 6.28–7.67 (m, 16H, cis; 16H, trans); ^{13}C (75 MHz, $CDCl_3$) δ 19.5 (q), 20.6 (q), 20.9 (q), 21.2 (q), 29.1 (t), 29.6 (t), 29.9 (t), 30.1 (t), 116.0 (d), 116.2 (d), 116.83 (d), 116.86 (d), 122.3 (d), 123.0 (d), 124.11 (d), 124.17 (d), 124.4 (d), 124.6 (d), 124.8 (s), 125.0 (s), 125.2 (s), 125.77 (d), 125.80 (s), 125.95 (d), 126.07 (d), 126.6 (d), 126.7 (s), 126.8 (d), 127.2 (d), 127.4 (d), 127.5 (d), 127.7 (d), 127.82 (d), 127.85 (d), 128.1 (d), 128.2 (d), 128.3 (d), 128.5 (d), 128.8 (d), 129.2 (d), 130.4 (s), 130.8 (s), 131.5 (s), 132.0 (s), 134.3 (s), 135.3 (s), 135.6 (s), 135.98 (s), 136.0 (s), 136.2 (s), 126.3 (s), 136.6 (s), 140.7 (s), 141.1 (s), 152.4 (s), 153.2 (s), 153.3 (s), 154.7 (s), due to strong overlap in the aromatic region five (d) and five (s) were not observed; *m*/*z* (EI, %)=482 (M^+,100); HRMS (EI) calcd for $C_{34}H_{26}OS$: 482.1704, found: 482.1695.

5.2.4. 2-(2,6-Dimethylphenyl)-9-(7′-methyl-2′,3′-dihydro-4′-(1′H)-phenanthren-4′-ylidene)-9H-xanthene (**5**)

Starting from episulfide **18** (120 mg, 0.24 mmol) using the standard procedure with *p*-xylene and copper powder, the alkene **5** (100 mg, 0.21 mmol, 89%) was obtained as a white solid after column chromatography (SiO_2, heptane/ethyl acetate=50:1); ^1H (300 MHz, $CDCl_3$) δ 0.79 (s, 3H, cis), 1.72 (s, 3H, cis), 1.85–2.39 (m, 3H, cis; 3H, trans), 2.06 (s, 3H, trans), 2.29 (s, 3H, trans), 2.35 (s, 3H, trans), 2.39 (s, 3H, cis), 3.00–3.10 (m, 2H, cis; 2H, trans), 3.54–3.58 (m, 1H, cis; 1H, trans), 6.26–6.27 (d, *J*=2.0 Hz, 1H, cis), 6.33–6.35 (m, 2H, trans), 6.69–6.71 (dd, *J*=8.3, 2.0 Hz, 1H), 6.81–6.82 (d, *J*=7.8 Hz, 1H), 6.87–7.48 (m, 10H, cis; 12H, trans), 7.57–7.59 (d, *J*=8.3 Hz, 1H, cis), 7.65–7.67 (d, *J*=8.3 Hz, 1H), 7.69–7.71 (d, *J*=7.3 Hz, 1H); ^{13}C (125 MHz, $CDCl_3$) δ 19.1 (q), 20.6 (q), 21.0 (q), 21.1 (q), 21.2 (q), 21.4 (q), 21.7 (t), 22.1 (t), 28.4 (t), 28.5 (t), 28.6 (t), 29.0 (t), 116.1 (d), 116.3 (d), 116.7 (d), 122.3 (d), 122.9 (d), 123.1 (s), 124.9 (d), 125.0 (d), 125.2 (s), 125.5 (s), 125.6 (s), 126.0 (s), 126.48 (d), 126.51 (d), 126.54 (d), 126.7 (d), 126.8 (d), 126.9 (d), 127.1 (d), 127.3 (d), 127.4 (d), 127.5 (d), 127.6 (d), 127.7 (d), 127.8 (d), 127.9 (d), 128.3 (d), 128.7 (d), 132.4 (s), 132.8 (s), 133.5 (s), 133.7 (s), 133.8 (s), 134.0 (s), 135.7 (s), 136.2 (s), 136.4 (s), 136.5 (s), 136.6 (s), 137.1 (s), 137.5 (s), 141.0 (s), 141.4 (s), 152.6 (s), 153.4 (s), 153.5 (s), 155.0 (s), due to strong overlap in the aromatic region seven (d) and six (s) were not observed; *m*/*z* (EI, %)=478 (M^+, 100); HRMS (EI) calcd for $C_{36}H_{30}O$: 478.2297, found: 478.2298.

5.2.5. 2-(2,6-Dimethylphenyl)-9-(2′,3′-dihydro-1′H-naphtho[2,1-b]pyran-1′-ylidene)-9H-xanthene (**6**)

Heating the episulfide **19** (50 mg, 0.10 mmol) in *p*-xylene at reflux in the presence of copper powder (200 mg) gave the alkene **6** as a slightly coloured oil. After purification by column chromatography the oil solidified and was obtained as a white solid after washing with small amounts of ether and ethyl acetate (42 mg, 0.09 mmol, 90%); ^1H (500 MHz, $CDCl_3$) δ 0.83 (s, 3H, cis), 1.70 (s, 3H, cis), 1.99 (s, 3H, trans), 2.25 (s, 3H, trans), 2.43–2.54 (m, 1H, cis), 2.56–2.67 (m, 1H, trans), 3.69–3.74 (m, 1H, trans), 3.77–3.82 (m, 1H, cis), 4.54–4.94 (m, 2H, cis; 2H, trans), 6.32–6.37 (m, 1H, trans), 6.52–6.53 (d, *J*=1.8 Hz, 1H, cis), 6.57–6.60 (dd, *J*=7.9, 1.3 Hz, 1H, trans), 6.72–6.75 (dd, *J*=8.3, 2.0 Hz, 1H, cis), 6.79–6.81 (d, *J*=7.3 Hz, 1H, trans), 6.86–7.69 (m, 14H, cis; 13H, trans); ^{13}C (75 MHz, $CDCl_3$) δ 19.5 (q), 20.6 (q), 20.9 (q), 21.2 (q), 29.1 (t), 29.5 (t), 69.3 (t), 69.6 (t), 116.4 (d), 116.6 (d), 116.9 (d), 117.0 (d), 118.4 (d), 118.8 (d), 118.9 (s), 119.2 (s), 122.3 (s), 122.5 (d), 122.7 (d), 122.8 (s), 122.9 (d), 123.0 (d), 124.50 (d), 124.53 (d), 125.3 (d), 125.6 (s), 125.8 (d), 125.95 (s), 126.03 (s), 126.3 (s), 126.4 (s), 126.6 (2×d), 126.7 (d), 126.8 (d), 126.9 (d), 127.3 (d), 127.4 (d), 127.42 (d), 127.47 (s), 127.6 (d), 127.7 (d), 128.0 (2×d), 128.1 (d), 128.2 (s), 128.3 (d), 128.7 (d), 128.8 (s), 128.9 (d), 129.3 (s), 129.8 (d), 129.9 (d), 135.8 (s), 136.1 (s), 136.2 (s), 136.3 (s), 136.3 (s), 136.6 (s), 140.7 (s), 141.2 (s), 152.7 (s), 153.6 (s), 153.6 (s), 154.1 (s), 154.2 (s), 155.2 (s), one carbon (s) was not observed; *m*/*z* (EI, %)=466 (M^+, 100); HRMS (EI) calcd for $C_{34}H_{26}O_2$: 466.1933, found: 466.1924.

5.2.6. 2-Bromo-xanthen-9-one (**12**)

This compound was prepared according to a two step literature procedure[18] from which the desired **12** was obtained as a white solid; mp 149.3–150.5 °C (lit. 150 °C); ^1H (300 MHz, $CDCl_3$) δ 7.38–7.43 (m, 2H), 7.49–7.51 (d, *J*=8.4 Hz, 1H), 7.73–7.82 (m, 2H), 8.32–8.35 (dd, *J*=7.8, 1.6 Hz, 1H), 8.45–8.46 (d, *J*=2.6 Hz, 1H); ^{13}C (75 MHz, $CDCl_3$) δ 116.9 (s), 117.9 (d), 119.9 (d), 121.3 (s), 122.9 (s), 124.2 (d), 126.6 (d), 129.0 (d), 135.1 (d), 137.5 (d), 154.7 (s), 155.8 (s), 175.7 (s); *m*/*z* (EI, %)=276 (M^+, 97), 274 (M^+, 100), 139 (42); HRMS (EI): calcd for $C_{13}H_7^{79}BrO_2$: 273.9629, found: 273.9626.

5.2.7. 2-(2,6-Dimethylphenyl)-9H-xanthen-9-one (**14**)

A solution of ketone **12** (1.2 g, 4.0 mmol) and $Pd(PPh_3)_4$ (190 mg, 0.16 mmol, 4 mol%) in DME (30 ml) was stirred under an argon atmosphere for 30 min. Then were added 2,6-dimethylphenylboronic acid (0.80 g, 5.2 mmol), $Ba(OH)_2 \cdot 8H_2O$ (2.7 g, 8.6 mmol) and water (30 ml). The resulting mixture was heated overnight at reflux. Water was added and the reaction mixture was extracted with ether (3×50 ml). The combined organic layers were dried over $MgSO_4$ prior to removal of the solvent under reduced pressure. The sticky beige solid obtained was then purified by column chromatography (SiO_2, heptane/ethyl acetate=16:1, R_f=0.5) providing ketone **14** as a white solid (0.93 g, 3.1 mmol, 78%, mp 133.0–134.2 °C); ^1H (300 MHz, $CDCl_3$) δ 2.05 (s, 6H), 7.13–7.78 (m, 8H), 8.17 (d, *J*=1.8 Hz, 1H), 8.36–8.39 (dd, *J*=7.9, 1.3 Hz, 1H); ^{13}C (75 MHz, $CDCl_3$) δ 20.7 (q), 117.7 (d), 118.0 (d), 121.6 (s), 123.7 (d), 126.4 (d), 126.6 (d), 127.3 (d), 134.6 (d), 135.77 (s), 135.78 (d), 136.7 (s), 139.8 (s), 154.8 (s), 155.9 (s), 176.9 (s), one carbon (s) was not observed due to overlap in the spectrum; *m*/*z* (EI, %)=300 (M^+, 100), 299 (62); HRMS (EI) calcd for $C_{21}H_{16}O_2$: 300.1150, found: 300.1140. Ele. Anal., calcd (%): C, 83.98; H, 5.37. Found (%): C, 83.82; H, 5.44.

5.2.8. 2-(2,6-Dimethylphenyl)-9H-xanthene-9-thione (**11**)

Ketone **14** (0.82 g, 2.70 mmol) was heated at reflux overnight in a suspension of P_4S_{10} (2.0 g, 4.5 mmol) in toluene (25 ml). The suspension was then filtered and the residues washed with CH_2Cl_2. The organic volatiles were removed under reduced pressure yielding a brownish solid, which was purified by column chromatography (SiO_2, heptane/ethyl acetate=50:1, R_f=0.6) giving the pure thioketone **11** as tiny green needles (0.72 g, 2.28 mmol, 84%, mp 109.7–110.7 °C); ^1H (300 MHz, $CDCl_3$) δ 2.07 (s, 6H), 7.13–7.23 (m, 3H), 7.36–7.41 (m, 1H), 7.52–7.58 (m, 3H), 7.75–7.80 (m, 1H), 8.57 (s, 1H), 8.74–8.77 (d, *J*=8.1 Hz, 1H); ^{13}C (75 MHz, $CDCl_3$) δ 21.0 (q), 118.1 (d), 118.3 (d), 124.6 (d), 127.4 (d), 128.9 (s), 129.7 (d), 129.9 (d), 134.7 (d), 135.9 (s), 136.0 (d), 137.5 (s), 139.9 (s), 149.2 (s), 150.3 (s), 204.4 (s), one (s)

and one (d) were not observed; *m*/*z* (EI, %)=316 (M^+, 100), 315 (70); HRMS (EI): calcd for $C_{21}H_{16}OS$: 316.09219, found 316.098. Ele. Anal., calcd (%): C, 79.71; H, 5.10. Found (%): C, 79.55; H, 4.89.

5.3. General procedure for the synthesis of thiiranes (episulfides) (15–19)

To a solution of hydrazone **9** (200 mg, 0.94 mmol) in CH_2Cl_2 (10 ml) under a nitrogen atmosphere were subsequently added $MgSO_4$ (300 mg), Ag_2O (200 mg) and a saturated solution of KOH in methanol (10 drops) at 0 °C. Stirring this mixture for 30 min at 0 °C gave a dark red solution. More Ag_2O and KOH in methanol were added if only a slightly red colour was observed. The solution was then filtered into another ice-cooled flask after which a solution of the appropriate thioketone in CH_2Cl_2 was added. Most of the time, the evolution of nitrogen gas could be observed. Stirring was continued for 2 h at 0 °C and then for 4 h at room temperature. Evaporation of the CH_2Cl_2 gave a black residue that was further purified by column chromatography.

*5.3.1. Dispiro[7-methyl-2,3-dihydro-4(1H)-phenanthrene-4,2′-thiirane-3′,9″-[2″-(2,6-dimethylphenyl)-9″H-thioxanthene]] (**15**)*

Starting from the hydrazone **8** (200 mg, 0.89 mmol) and thioketone **10** a cis–trans mixture in a nearly 1:1 ratio of episulfides **15** was obtained as a slightly yellow foam after column chromatography (SiO_2, heptane/ethyl acetate=50:1) (80 mg, 0.15 mmol, 17%, based on the used hydrazone **8**). The cis–trans mixture of episulfides **15** was used immediately in the next step; *m*/*z* (EI, %)=526 (M^+, 12), 494 (30), 256 (83), 160 (51), 128 (60), 64 (100); HRMS (EI) calcd for $C_{36}H_{30}S_2$: 526.1789, found: 526.1783.

*5.3.2. Dispiro[2,3-dihydro-1H-naphtho[2,1-b]pyran-1,2′-thiirane-3′,9″-[2″-(2,6-dimethylphenyl)-9″H-thioxanthene]] (**16**)*

Starting from hydrazone **9** (200 mg, 0.74 mmol) and thioketone **10**, thiirane **16** was obtained as a slightly yellow foam after column chromatography (SiO_2, hexane/ethyl acetate=50:1) as a mixture of cis- and trans-isomers (150 mg, 0.29 mmol, 31% based on hydrazone **9**), which was not further separated into its isomers, but directly used in the next step; *m*/*z* (EI, %)=514 (M^+, 12), 482 (100); HRMS (EI) calcd for $C_{34}H_{26}OS_2$: 514.1425, found: 514.1409.

*5.3.3. Dispiro[2,3-dihydro-1H-naphtho[2,1-b]thiopyran-1,2′-thiirane-3′,9″-[2″-(2,6-dimethylphenyl)-9″H-xanthene]] (**17**)*

Reaction of hydrazone **7** (100 mg, 0.44 mmol) with thioketone **11** in the standard way gave after column chromatography (SiO_2, heptane/ethyl acetate=50:1) the thiirane **17** as a cis–trans mixture (140 mg, 0.27 mmol, 72% based on hydrazone). This mixture was not separated, but directly used in the next step; *m*/*z* (EI, %)=514 (M^+, 15), 482 (100), 298 (19); HRMS (EI) calcd for $C_{34}H_{26}OS_2$: 514.1425, found: 514.1517.

*5.3.4. Dispiro[7-methyl-2,3-dihydro-4(1H)-phenanthrene-4,2′-thiirane-3′,9″-[2″-(2,6-dimethylphenyl)-9″H-xanthene]] (**18**)*

Hydrazone **8** (200 mg, 0.89 mmol) and thioketone **11** (180 mg, 0.56 mmol) were allowed to react according to the standard procedure providing episulfide **18** (220 mg, 0.43 mmol, 77% based on thioketone). Purification was performed by column chromatography (SiO_2, hexane/ethyl acetate=50:1); *m*/*z* (EI, %)=510 (M^+, 18), 478 (100), 285 (41); HRMS (EI) calcd for $C_{36}H_{30}OS$: 510.2017, found: 510.2018.

*5.3.5. Dispiro[2,3-dihydro-1H-naphtho[2,1-b]pyran-1,2′-thiirane-3′,9″-[2″-(2,6-dimethylphenyl)-9″H-xanthene]] (**19**)*

Hydrazone **9** (100 mg, 0.47 mmol) and thioketone **11** (100 mg, 0.32 mmol) were used to synthesize episulfide **19** (120 mg, 0.24 mmol, 67% based on thioketone). Purification was performed by column chromatography (SiO_2, hexane/ethyl acetate=50:1). The cis–trans mixture obtained was not separated but directly used in the next step; *m*/*z* (EI, %)=498 (M^+, 100), 466 (100); HRMS (EI) calcd for $C_{34}H_{26}O_2S$: 498.1653, found: 498.1647.

Supplementary data

Supplementary data associated with this article can be found in the online version, at doi:10.1016/j.tet.2009.03.081.

References and notes

1. (a) Venturi, M.; Credi, A.; Balzani, V. *Molecular Devices and Machines—A Journey into the Nanoworld*; Wiley-VCH: Weinheim, 2003; (b) Sauvage, J. P. *Struct. Bond.* **2001**, *99*, 55–78; (c) Balzani, V.; Credi, A.; Raymo, F. M.; Stoddart, J. F. *Angew. Chem., Int. Ed.* **2000**, *39*, 3348–3391; (d) Feringa, B. L.; Koumura, N.; Delden, R. A. v.; Wiel, M. K. J. t. *Appl. Phys. A.* **2002**, *75*, 301–308; (e) Kinbara, K.; Aida, T. *Chem. Rev.* **2005**, *105*, 1377–1400.
2. (a) Browne, W. R.; Feringa, B. L. *Nat. Nanotechnol.* **2006**, *1*, 25–35; (b) Feringa, B. L. *J. Org. Chem.* **2007**, *72*, 6635–6652.
3. Diederich, F. *Angew. Chem., Int. Ed.* **2007**, *46*, 68–69; *Angew. Chem.* **2007**, *119*, 68–70.
4. Kay, E. R.; Leigh, D. A.; Zerbetto, F. *Angew. Chem., Int. Ed.* **2007**, *46*, 72–191; *Angew. Chem.* **2007**, *119*, 72–196.
5. Saha, S.; Stoddart, J. F. *Chem. Soc. Rev.* **2007**, *36*, 77–92.
6. Kottas, G. S.; Clarke, L. I.; Horinek, D.; Michl, J. *Chem. Rev.* **2005**, *105*, 1281–1376.
7. (a) Koumura, N.; Zijlstra, R. W. J.; Delden, R. A. v.; Harada, N.; Feringa, B. L. *Nature* **1999**, *401*, 152–155; (b) Kelly, T. R.; De Silva, H.; Silva, R. A. *Nature* **1999**, *401*, 150–152; (c) Leigh, D. A.; Wong, J. K. Y.; Dehez, F.; Zerbetto, F. *Nature* **2003**, *424*, 174–179; (d) Hernández, J. V.; Kay, E. R.; Leigh, D. A. *Science* **2004**, *306*, 1532–1537.
8. Badjic, J. D.; Balzani, V.; Credi, A.; Silvi, S.; Stoddart, J. F. *Science* **2004**, *303*, 1845–1849.
9. Jiménez, M. C.; Dietrich-Buchecker, C.; Sauvage, J.-P. *Angew. Chem., Int. Ed.* **2000**, *39*, 3284–3287.
10. Muraoka, T.; Kinbara, K.; Kobayashi, Y.; Aida, T. *J. Am. Chem. Soc.* **2003**, *125*, 5612–5613.
11. (a) Dominguez, Z.; Dang, H.; Strouse, M. J.; Garcia-Garibay, M. A. *J. Am. Chem. Soc.* **2002**, *124*, 2398–2399; (b) Godinez, C. E.; Zepeda, G.; Garcia-Garibay, M. A. *J. Am. Chem. Soc.* **2002**, *124*, 4701–4707; (c) Dominguez, Z.; Dang, H.; Strouse, M. J.; Garcia-Garibay, M. A. *J. Am. Chem. Soc.* **2002**, *124*, 7719–7727; (d) Dominguez, Z.; Khuong, T.-A. V.; Dang, H.; Sanrame, C. N.; Nuñez, J. E.; Garcia-Garibay, M. A. *J. Am. Chem. Soc.* **2003**, *125*, 8827–8837.
12. (a) Koumura, N.; Geertsema, E. M.; Meetsma, A.; Feringa, B. L. *J. Am. Chem. Soc.* **2000**, *122*, 12005–12006; (b) Koumura, N.; Geertsema, E. M.; Gelder, M. B. v.; Meetsma, A.; Feringa, B. L. *J. Am. Chem. Soc.* **2002**, *124*, 5037–5051; (c) ter Wiel, M. K. J.; van Delden, R. A.; Meetsma, A.; Feringa, B. L. *J. Am. Chem. Soc.* **2003**, *125*, 15076–15086; (d) ter Wiel, M. K. J.; van Delden, R. A.; Meetsma, A.; Feringa, B. L. *J. Am. Chem. Soc.* **2005**, *127*, 14208–14222; (e) van Delden, R. A.; ter Wiel, M. K. J.; Pollard, M. M.; Vicario, J.; Koumura, N.; Feringa, B. L. *Nature* **2005**, *437*, 1337–1340.
13. Jager, W. F.; de Jong, J. C.; de Lange, B.; Huck, N. M. P.; Meetsma, A.; Feringa, B. L. *Angew. Chem., Int. Ed. Engl.* **1995**, *34*, 348–350.
14. ter Wiel, M. K. J.; van Delden, R. A.; Meetsma, A.; Feringa, B. L. *Org. Biomol. Chem.* **2005**, *3*, 4071–4076.
15. Schoevaars, A. M.; Kruizinga, W.; Zijlstra, R. W. J.; Veldman, N.; Spek, A. L.; Feringa, B. L. *J. Org. Chem.* **1997**, *62*, 4943–4948.
16. Feringa, B. L.; Jager, W. F.; de Lange, B.; Meijer, E. W. *J. Am. Chem. Soc.* **1991**, *113*, 5468–5470.
17. de Lange, B. Chiroptical Molecular Switches, Ph.D. Thesis; Rijksuniversiteit Groningen, 1993.
18. Dhar, S. N. *J. Chem. Soc.* **1920**, *117*, 1053–1070.
19. ter Wiel, M. K. J.; Vicario, J.; Davey, S. G.; Meetsma, A.; Feringa, B. L. *Org. Biomol. Chem.* **2005**, *3*, 28–30.
20. In the EXSY experiment the same pulse sequence is used as for the standard NOESY experiment. In the NOESY experiment polarization transfer occurs over a certain period of time (mixing time, t_m) by cross-polarization whereas the polarization transfer in an EXSY experiment occurs through a chemical exchange process. For all molecules considered in this chapter, the NOE-signals in the 2D spectra were negative and hence the observed EXSY-signals were positive; see for example: Bodenhausen, G.; Kogler, H.; Ernst, R. R. *J. Magn. Reson.* **1984**, *58*, 370–388.
21. According to the initial rate approximation method proposed by Ernst and coworkers, the rate of exchange (rate of rotation k) can be calculated directly from the ratio of cross- (a_{AB} and a_{BA}) and autopeak integrations (a_{AA} and a_{BB}) and the mixing time using the formula $(a_{AA}/a_{AB})=(1-kt_m)/kt_m$, provided a slow exchange situation and absence of scalar spin-spin coupling. This equation can be transformed into to $k=1/t_m(a_{AB}/(a_{AA}+a_{AB}))$. A plot of t_m versus $(a_{AB}/(a_{AA}+a_{AB}))$ will therefore directly give the rate constant k at a given temperature. These k-values can be used subsequently to determine of the thermodynamic constants, $\Delta^{\ddagger}G^{\theta}$, $\Delta^{\ddagger}H^{\theta}$ and $\Delta^{\ddagger}S^{\theta}$, via an Eyring plot ($\ln(kh/k_bT)$ vs $1/T$): (a) Jeener, J.; Meier, B. H.; Bachmann, P.; Ernst, R. R. *J. Chem. Phys.* **1979**, *71*, 4546–4553; (b) Macura, S.;

Ernst, R. R. *Mol. Phys.* **1980**, *41*, 95–117; (c) Bodenhausen, G.; Ernst, R. R. *J. Am. Chem. Soc.* **1982**, *104*, 1304–1309.
22. Exchange at 15 °C proceeded too slowly to give accurate results.
23. The actual mixing times used per rotor are depicted in Supplementary data.
24. It is hard to depict the rate constants in a graphical way and their differences cannot be appreciated well. They are therefore depicted numerically in Supplementary data.
25. Jager, W.F. Chiroptical Molecular Switches, Ph. D. Thesis; Rijksuniversiteit Groningen, 1994.
26. (a) Smid, W. I.; Schoevaars, A. M.; Kruizinga, W.; Veldman, N.; Smeets, W. J. J.; Spek, A. L.; Feringa, B. L. *Chem. Commun.* **1996**, 2265–2266; (b) ter Wiel, M. K. J.; Meetsma, A.; Feringa, B. L. *Tetrahedron* **2002**, *58*, 2183–2188.
27. Bax, A.; Freeman, R. *J. Magn. Reson.* **1981**, *44*, 542–561.
28. Bax, A.; Davis, D. G. *J. Magn. Reson.* **1985**, *65*, 355–360.
29. Bax, A.; Griffey, R. H.; Hawkins, B. L. *J. Magn. Reson.* **1983**, *55*, 301–315.
30. For an overview of NMR techniques see: (a) Sanders, J. K. M.; Hunter, B. *Modern NMR Spectroscopy; A Guide for Chemists*; Oxford University Press: Oxford, 1987; (b) Croasmun, W. R.; Carlson, R. M. N. *Two Dimensional NMR Spectroscopy: Applications for Chemists and Biochemists*; VCH: New York, NY, 1987; (c) Friebolin, H. *Basic One- and Two Dimensional NMR Spectroscopy*; VCH: New York, NY, 1998; (d) Ernst, R. R.; Bodenhausen, G.; Wokaun, A. *Principles of Nuclear Magnetic Resonance Spectroscopy in One and Two Dimensions*; Clarendon: Oxford, 1987; (e) Harris, R. K. *Nuclear Magnetic Resonance Spectroscopy, a Physicochemical View*; Longman: Harlow, 1991.
31. Marion, D.; Wuthrich, K. *Biochem. Biophys. Res. Commun.* **1983**, *113*, 967–974.
32. (a) Willem, R. *Prog. NMR Spectrosc.* **1987**, *20*, 1–94; (b) Orrell, K. G.; Sik, V.; Stephenson, D. *Prog. NMR Spectrosc.* **1990**, *22*, 141–208.
33. (a) Kuchel, P. W.; Bulliman, B. T.; Chapman, B. E.; Mendz, G. L. *J. Magn. Reson.* **1988**, *76*, 136–142; (b) Perrin, C. L. *J. Magn. Reson.* **1989**, *82*, 619–621.